

# Polarization: BICEP-II $\rightarrow$ Planck

Jim Rich

SPP-IRFU  
CEA-Saclay  
91191 Gif-sur-Yvette  
[james.rich@cea.fr](mailto:james.rich@cea.fr)

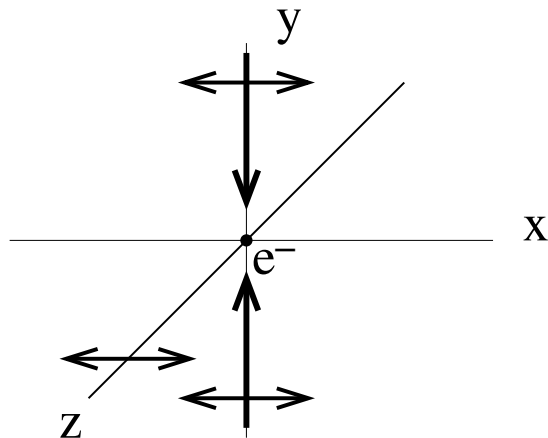
April 8, 2014

# Outline

- Generation of polarization of microwave radiation
  - Thomson scattering
  - Spinning dust
- E and B modes
- Bicep-II (PRL 112,241101)
- Planck XIX (arXiv:1405.0871)
- Planck XXX (arXiv:1409.5738)

# Thomson scattering polarizes photons

Compton scattering just before recombination;  
LSS= $xy$ -plane; Observer on  $z$  axis

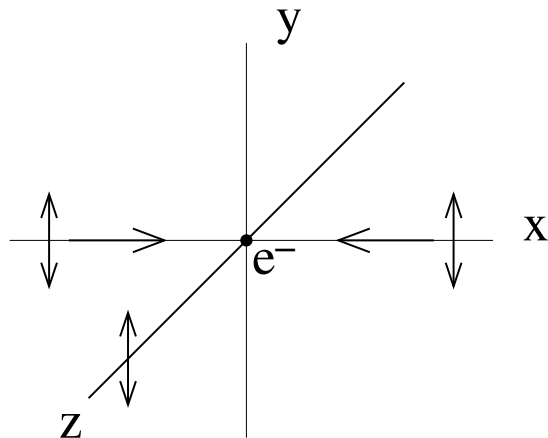


photon flux( $\pm y$  directions)

$\Rightarrow$  photon polarization observed in  $x$  direction

# Thomson scattering polarizes photons

Compton scattering just before recombination;  
LSS= $xy$ -plane; Observer on  $z$  axis

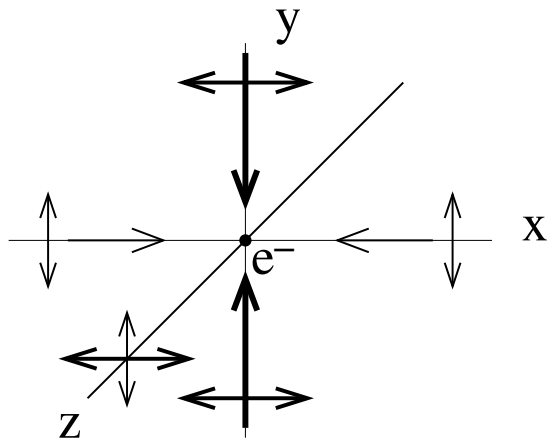


photon flux( $\pm x$  directions)

$\Rightarrow$  photon polarization observed in  $y$  direction

## Inhomogeneities $\Rightarrow$ linear polarization

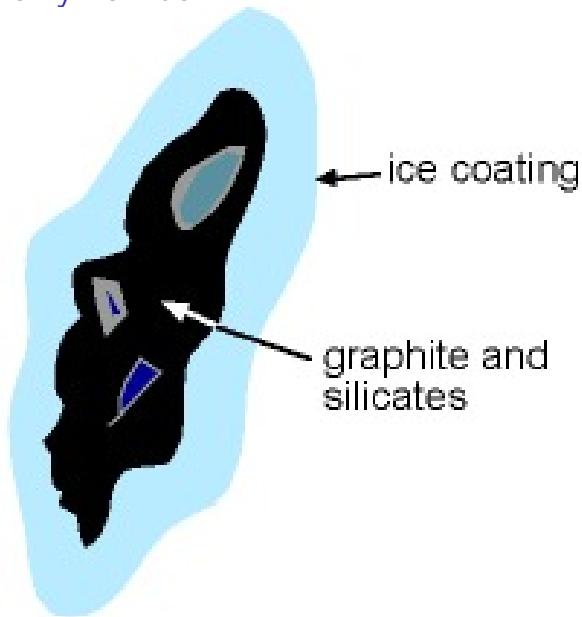
Compton scattering just before recombination;  
LSS= $xy$ -plane; Observer on  $z$  axis



photon flux( $\pm y$  directions)  $>$  photon flux( $\pm x$  directions)  
 $\Rightarrow$  photon polarization observed in  $x$  direction

## 19.6K dust: Cosmo enemy number 1

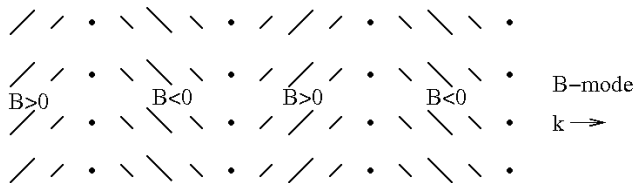
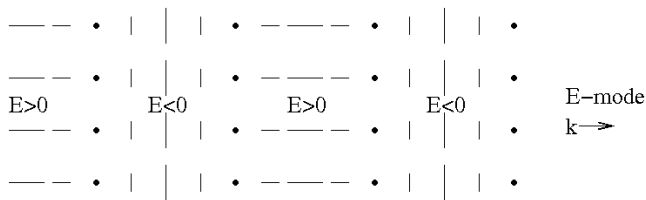
100  
nanometers



## Polarization from dust (Planck Int. Res. XIX)

The linear polarization of the thermal dust emission arises from a combination of two main factors. Firstly, a fraction of the dust grain population is **non-spherical**, and this gives rise to **different emissivities for radiations with the electric vector parallel or orthogonal to a grain's long axis**. Secondly, the **rotating grains are aligned by the interstellar magnetic field**, probably with differing efficiencies depending on grain size and composition [DraineFraissee2009]. While the details of this process remain unclear [Lazarian2003,Lazarian2007], there is a consensus that **the angular momentum of a grain spun up by photon-grain interactions** [Dolginov1976, DraineWeingartner96, DraineWeingartner1997, LazarianHoang2007, HoangLazarian2008] **becomes aligned with the grain's short axis, and then with the magnetic field via precession** [Martin71]. The end result is that, if we look across magnetic field lines, the rotating grain will have its long axis orthogonal to the field lines, and accordingly dust emission will be **linearly polarized with its electric vector normal to the sky-projected magnetic field**.

# Decompose polarization maps into E and B modes



- CMB scalar perturbations  $\rightarrow$  E modes
- CMB tensor perturbations  $\rightarrow$  E and B modes  $\ll$  scalar perturbations
- Dust  $\rightarrow$  E and B modes (roughly equal proportions)



# BICEP-II: Observations + Analysis

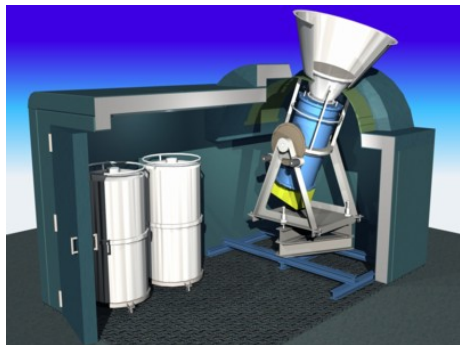
P.A.R Ade et al, arXiv:1403.3985

117 citations (March 18-April 8)

- Telescope and focal plane
- Observational strategy
- Timeline  $\rightarrow$  map
- Map  $\rightarrow$  power spectrum
- Jackknife search for systematics
- Corrections and Deprojections
- Foregrounds
- Cross-correlations

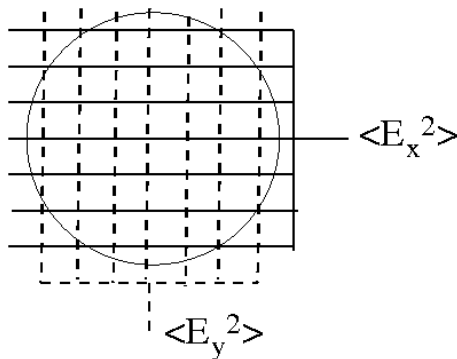
# Telescope

- 26cm refractor
- altitude-azimuthal-deck mount
- in helium cryostat
- 20degree field-of-view
- 0.5degree fwhm angular resolution



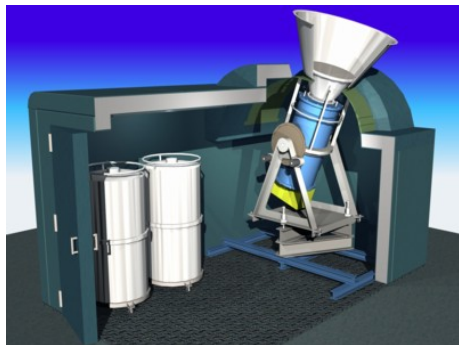
# Focal plane

- 256 dual-polarization pixels
- TES bolometers
- squid readout
- 150Ghz only
- each pixel sees 0.5deg

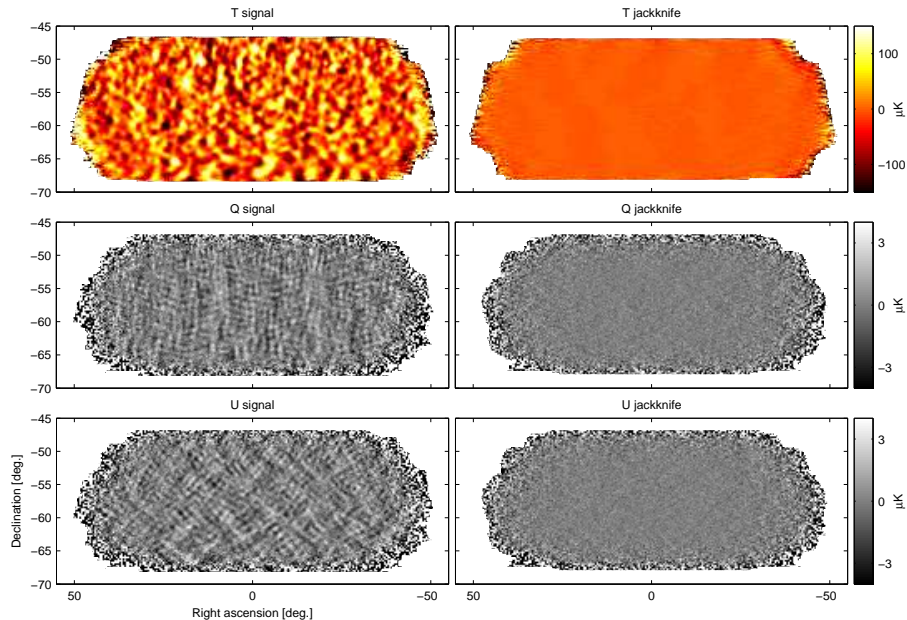


# Observations

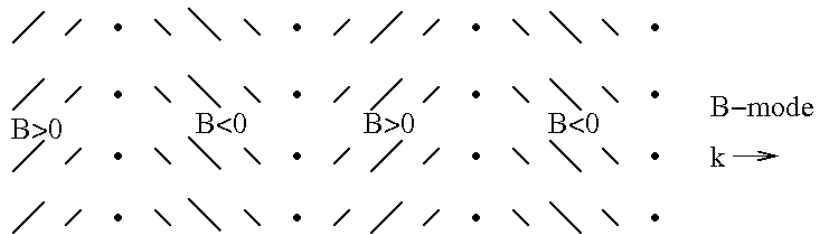
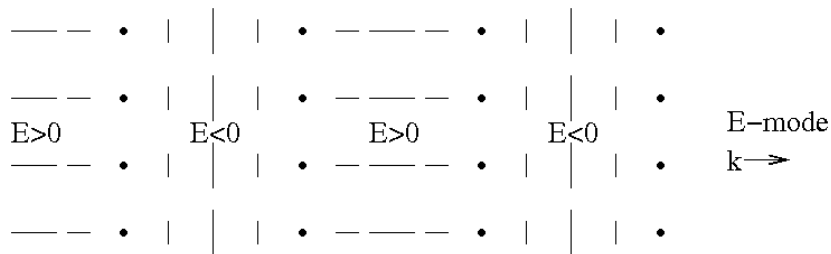
- Scan in azimuth:  $2.8\text{deg}/\text{sec}$ ; 56 times
- Change altitude by  $0.25\text{deg}$
- continue for 3 days to scan  $380\text{sqdeg}$  field
- change deck angle and repeat
- repeat cycle for 2years



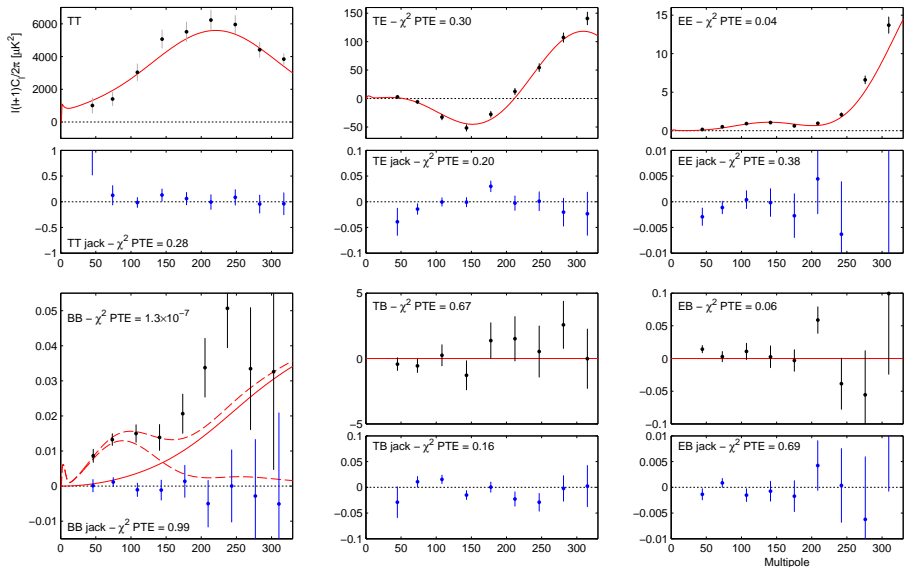
# Timeline $\rightarrow$ filter $\rightarrow$ Maps



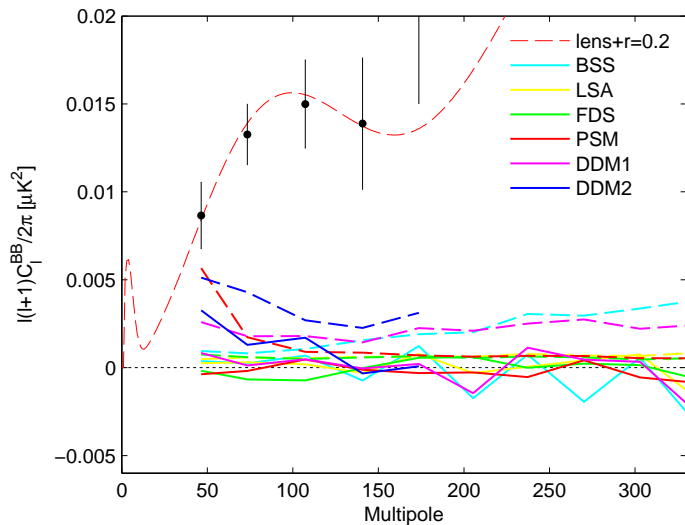
## Decompose maps into E and B modes



# Maps $\rightarrow$ power spectra

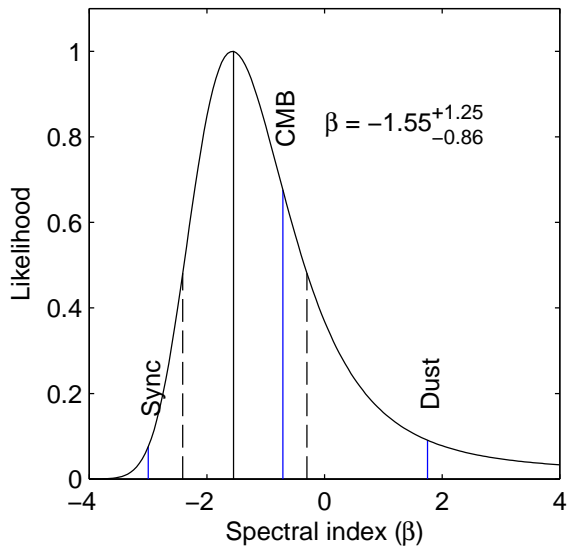


# Model B-mode foregrounds (dust)

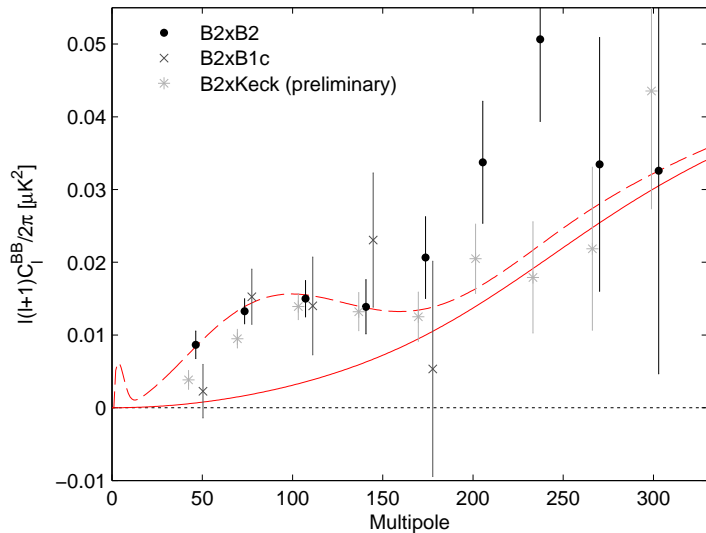




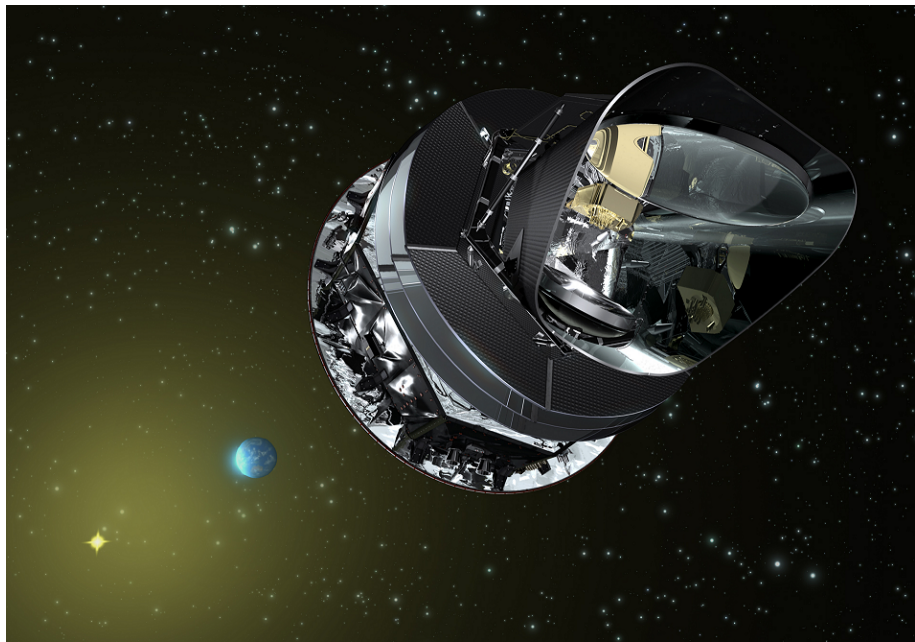
# Spectral index from Bicep II cross Bicep-I(100Mhz)



# Compare Bicep-II BB with cross correlations



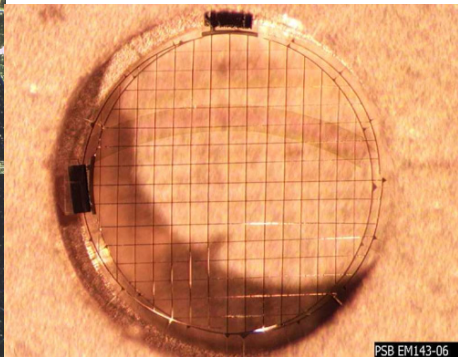
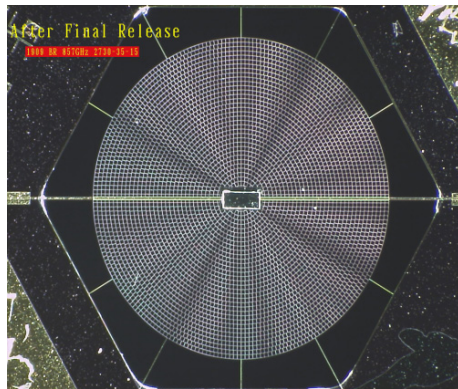
# Planck



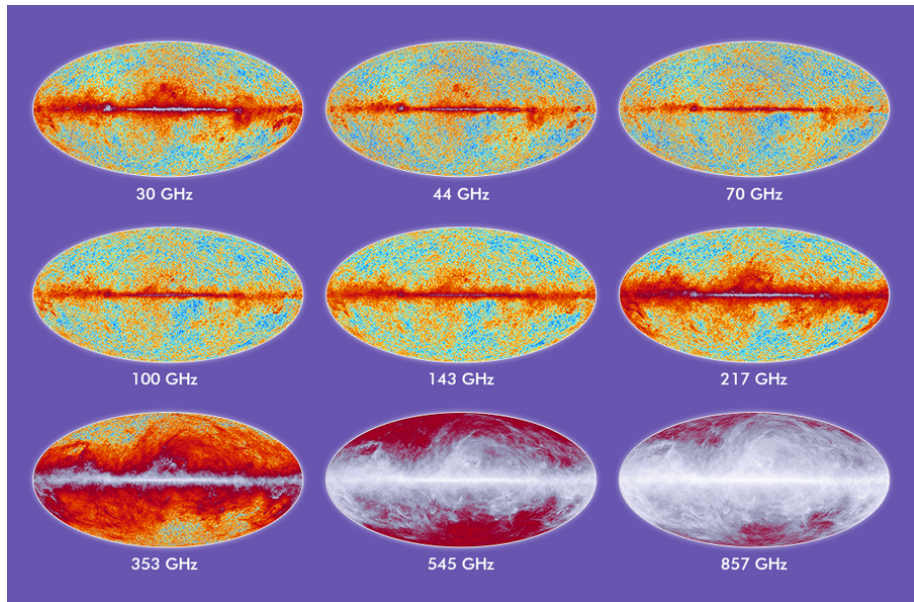
# Planck focal plane



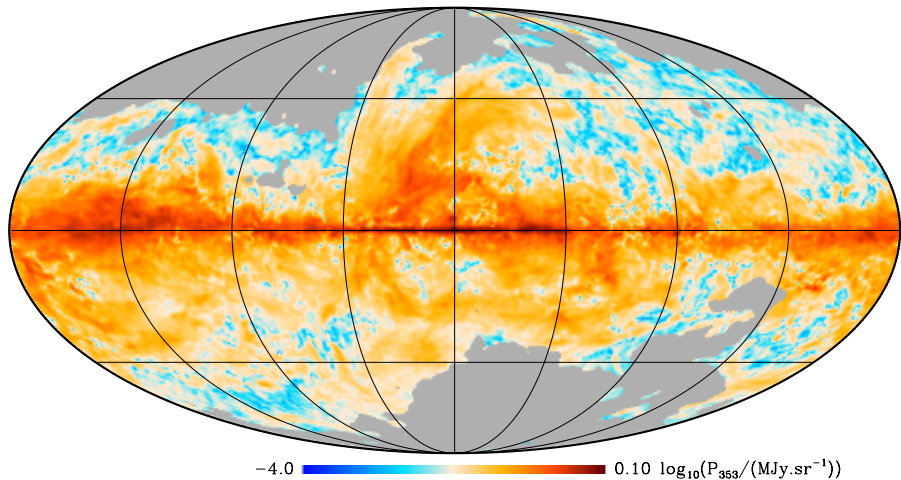
# Planck Bolometers



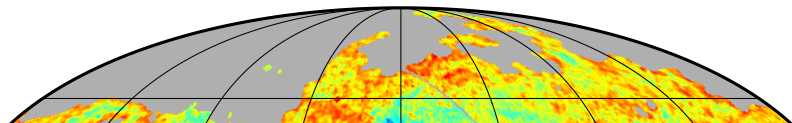
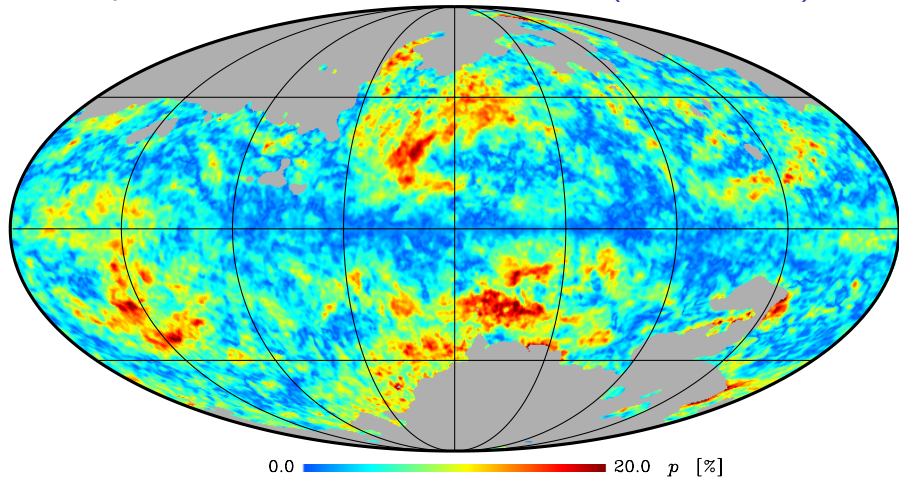
# Planck sky vs. frequency



# Planck polarization intensity at 353Ghz (Planck XIX)

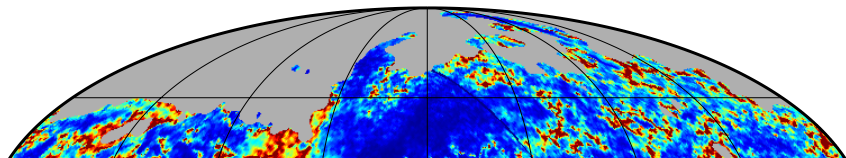
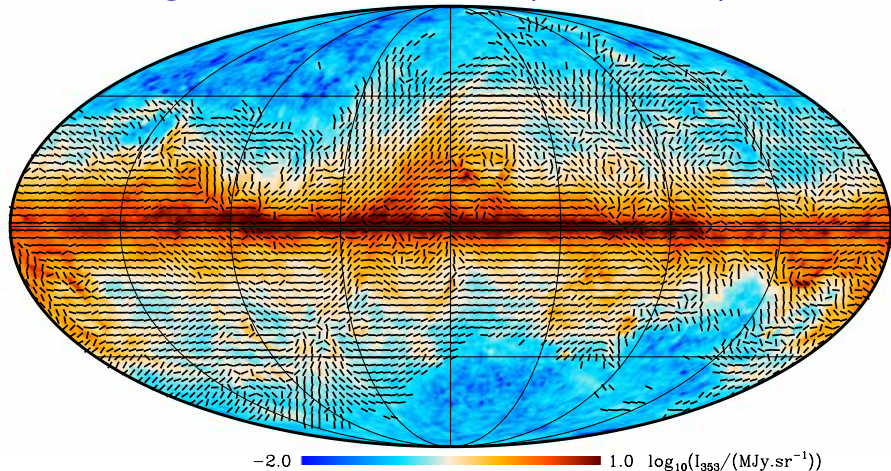


# Planck polarization fraction at 353Ghz (Planck XIX)





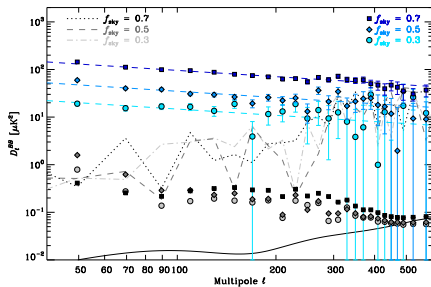
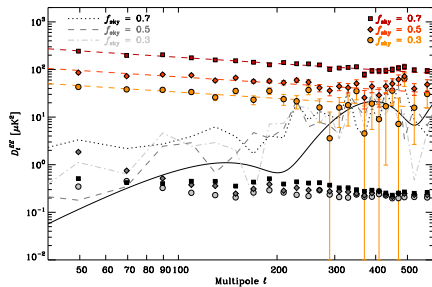
# Planck Magnetic field orientation (Planck XIX)



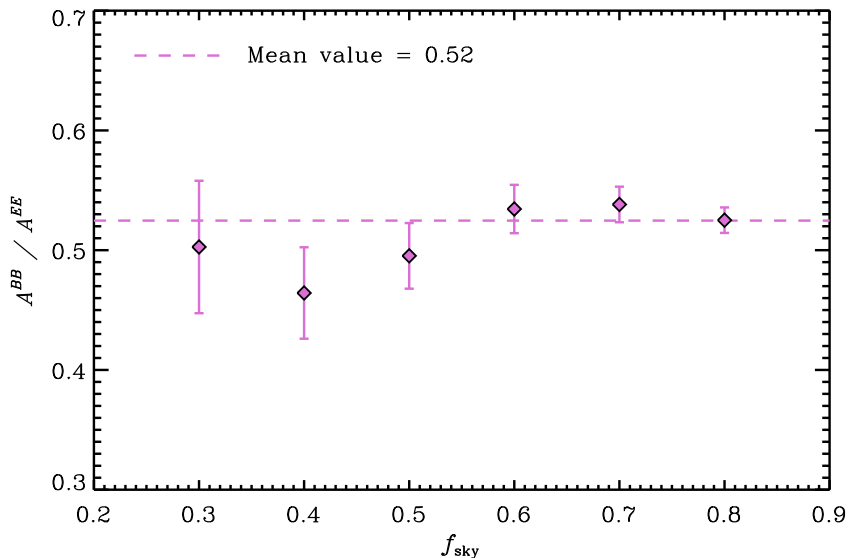
## Planck XIX (1405.0871) $\rightarrow$ XXX (1409.5738)

- Systematics improved
  - ADC nonlinearity
  - Corrections for “very long time constants”
- Main remaining systematic: intensity-to-polarization leakage
- Bright radio sources masked
- Maps derived from cross-correlation of two independent data sets (uncorrelated noise)
- Various null tests to search for systematics

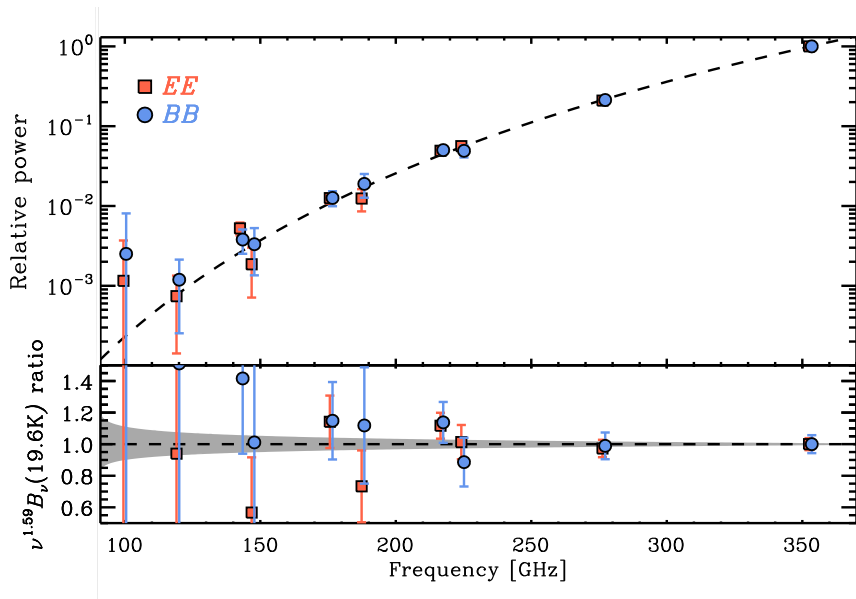
# High latitude EE and BB at 353GHz (Planck XXX)



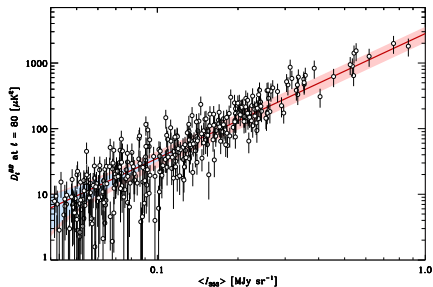
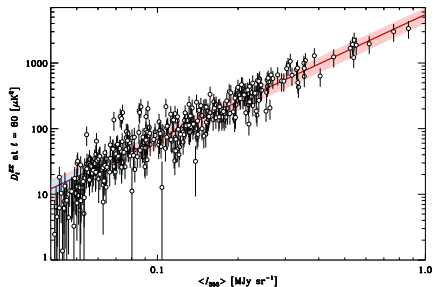
# BB/EE=0.52 at 353GHz (Why?)



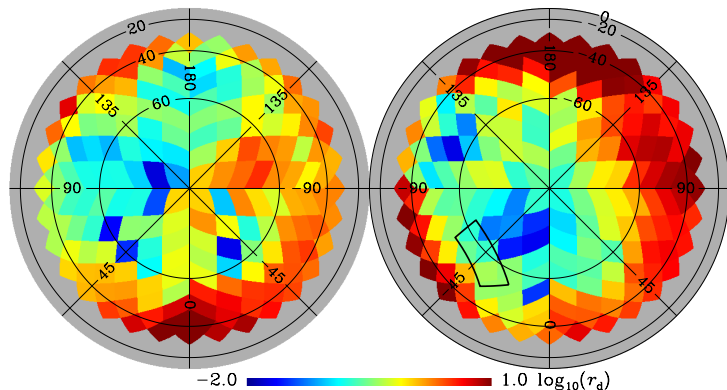
# EE and BB frequency dependence



# EE and BB ( $\ell = 80$ ) vs $I_{353}$ (400deg<sup>2</sup> patches)



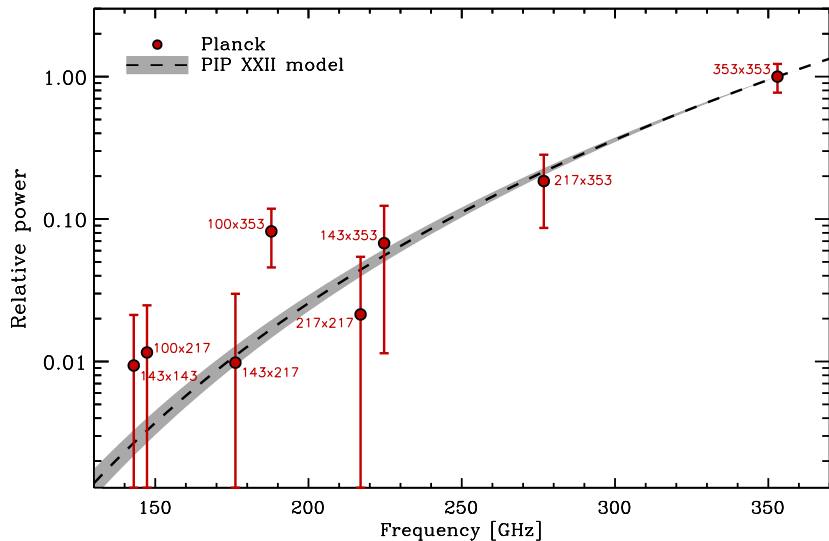
## BB in $400\text{deg}^2$ patches at 150GHz



$r_d$  = effective  $r$  from dust. ( $r_{BICEPS} \sim 0.2$ )

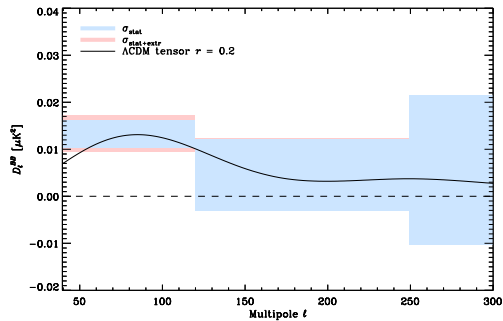
Cleanest patches have:  $r_d = 0.053 \pm 0.096$ ,  $0.027 \pm 0.098$ ,  
 $-0.062 \pm 0.052$ ,  $-0.020 \pm 0.127$ ,  $0.057 \pm 0.122$ , and  $-0.031 \pm 0.121$ ,

# BB frequency dependence in Biceps zone

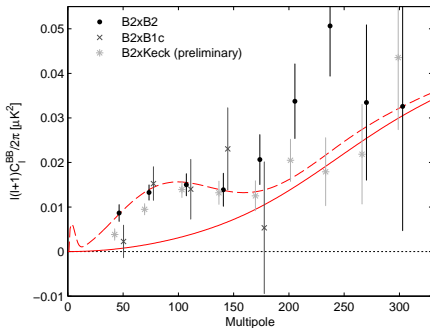
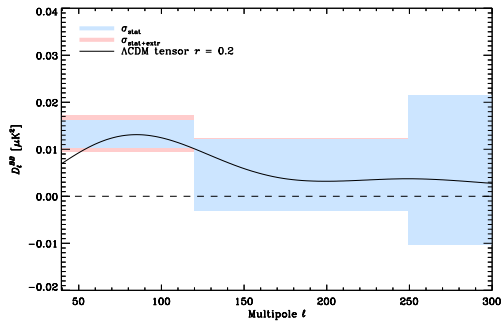




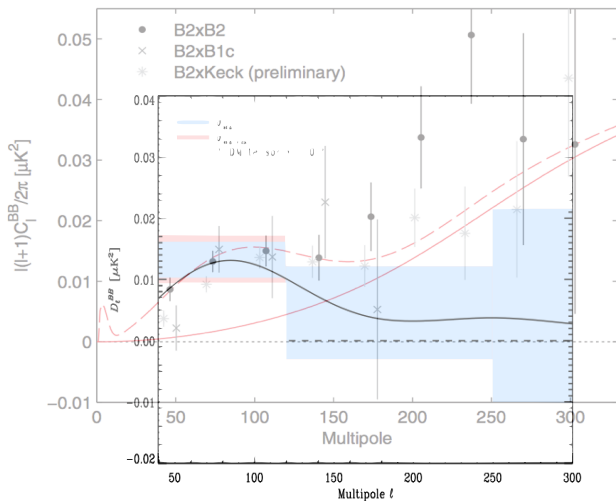
# Dust BB spectrum (150MHz) near Bicep-II field



# Dust BB spectrum (150MHz) near Bicep-II field



# Should be possible for BICEPS to see lensing B-modes



## Conclusions of XXX (general)

- The angular power spectra EE and BB at 353GHz are well fit by power laws in  $\ell$  with exponents consistent with  $\alpha = -2.42 \pm 0.02$ , for sky fractions ranging from 24% to 72% for the LR regions used.
- The amplitudes of  $D_\ell^{EE}$  and  $D_\ell^{BB}$  in the LR regions vary with mean dust intensity at 353 GHz,  $\langle I_{353} \rangle$ , roughly as  $\langle I_{353} \rangle^{1.9}$ .
- The frequency dependence of the dust  $D_\ell^{EE}$  and  $D_\ell^{BB}$  from 353 GHz down to 100 GHz, obtained after removal of the  $D_\ell^{EE}$  prediction from the Planck best-fit CMB model [planck2013-p11], is accurately described by the modified blackbody dust emission law derived in [planck2014-XXII], with  $\beta_d = 1.59$  and  $T_d = 19.6\text{K}$ .
- The ratio between the amplitudes of the two polarization power spectra is  $C_\ell^{BB} / C_\ell^{EE} = 0.53$ , which is not consistent with current theoretical models.
- Dust  $D_\ell^{EE}$  and  $D_\ell^{BB}$  spectra computed for 352 high Galactic latitude  $400 \text{ deg}^2$  patches satisfy the above general properties at 353 GHz and have the same frequency dependence.

## Conclusions (Background for CMB Polarization)

- Extrapolating the Planck 353GHz  $D_\ell^{BB}$  spectra computed on the  $400 \text{ deg}^2$  circular patches at high Galactic latitude to 150 GHz shows that we expect significant contamination by dust over most of the high Galactic latitude sky in the  $\ell$  range of interest for detecting a primordial  $D_\ell^{BB}$  spectrum.
- Even for the cleanest of these regions, the Planck statistical error on the estimate of  $D_\ell^{BB}$  amplitude at  $\ell = 80$  for such small regions is at best 0.17 ( $3\sigma$ ) in units of  $r_d$ .
- Our results show that subtraction of polarized dust emission will be essential for detecting primordial  $B$ -modes at a level of around 0.1 or below.
- There is a significant dispersion of the polarization  $D_\ell^{BB}$  amplitude for a given dust total intensity. Choices of the cleanest areas of the polarized sky cannot be made accurately using the Planck total intensity maps alone.

## Conclusions (Background for CMB Polarization, cont.)

- Component separation, or template cleaning, can best be done at present with the Planck HFI 353GHz data, but the accuracy of such cleaning is limited by Planck noise in small fields. Ground-based or balloon-borne experiments should include dust channels at high frequency. Alternatively, if they intend to rely on the Planck data to remove the dust emission, they should optimize the integration time and area so as to have a similar signal-to-noise level for the CMB and dust power spectra.

## Conclusions for BICEP2

- Over the multipole range  $40 < \ell < 120$ , the Planck 353GHz  $D_\ell^{BB}$  power spectrum extrapolated to 150GHz yields a value  $1.32 \times 10^{-2} \mu\text{K}_{\text{CMB}}^2$ , with statistical error  $\pm 0.29 \times 10^{-2} \mu\text{K}_{\text{CMB}}^2$  and a further uncertainty  $(+0.28, -0.24) \times 10^{-2} \mu\text{K}_{\text{CMB}}^2$  from the extrapolation. This value is comparable in magnitude to the BICEP2 measurements at these multipoles that correspond to the recombination bump.
- The frequency dependence of  $D_\ell^{BB}$  across the Planck bands is consistent with the typical SED of dust polarization [planck2014-XXII].
- Assessing the dust contribution to the  $B$ -mode power measured by the BICEP2 experiment requires a dedicated joint analysis with Planck, incorporating all pertinent observational details of the two data sets, such as masking, filtering, and colour corrections.
- We have identified regions in which the dust polarization  $D_\ell^{BB}$  amplitude may be significantly lower, by about a factor of 2, than in the BICEP2 observing region.